Journal of Organometallic Chemistry, 419 (1991) 219–232
Elsevier Sequoia S.A., Lausanne
JOM 22093

Dimethylsulfide derivatives of $[Rh_6(CO)_{16}]$. Crystal structures of $[Rh_6(CO)_{15}(SMe_2)]$ and $[Rh_6(CO)_{12}(SMe_2)_4]$

Sirpa Rossi, Kauko Kallinen, Jouni Pursiainen, Tuula T. Pakkanen and Tapani A. Pakkanen

University of Joensuu, Department of Chemistry, P.O. Box 111, SF-80101 Joensuu (Finland)

(Received May 22nd, 1991)

Abstract

The decahexacarbonylhexarhodium cluster $[Rh_6(CO)_{16}]$ reacts with dimethylsulfide to give a series of substituted clusters $[Rh_6(CO)_{16-x}(SMe_2)_x]$, $x = 1–4$ (**1**–**4**). The crystal structures of **1** and **4** have been determined. The SMe_2 ligands replace terminal carbonyls, otherwise the cluster structure is maintained. The four sulfide ligands in **4** replace four carbonyl groups at Rh atoms in the same plane of the Rh_6 octahedron, with the SMe_2 groups lying alternately above and below this plane. The di- and tri-substituted species have been characterized by ir spectroscopy and elemental analysis. The reactivity of $[Rh_6(CO)_{12}(SMe_2)_4]$ toward hydrogen and carbon monoxide has been studied. Under CO it undergoes replacement of SMe_2 by carbon monoxide to afford $[Rh_6(CO)_{16}]$. In a corresponding reaction with H_2 $[Rh_6(CO)_{12}(SMe_2)_4]$ is converted into a mixture of **2**–**4**. Hydrogenation of 1-hexene using $[Rh_6(CO)_{12}(SMe_2)_4]$ as a catalysts precursor was observed at 60 °C with a highest rate of 2200 turnovers/h.

Introduction

Rhodium carbonyl clusters $[Rh_4(CO)_{12}]$ and $[Rh_6(CO)_{16}]$ undergo carbonyl substitution reactions with several nucleophilic ligands. The number of carbonyl groups replaced depends on the molar ratio of ligand used and the vigor of the reaction conditions, as well as on the steric requirements of the ligand.

The reactions between $[Rh_6(CO)_{16}]$ and PPh_3 have been studied [1–4]. Several substitution products were identified on the basis of IR-spectra and elemental analyses, but no X-ray crystal structures or NMR spectra were reported. With $P(OPh)_3$, restriction of coordination to a maximum of four phosphite ligands has been attributed to steric restrictions. The crystal structure of $[Rh_6(CO)_{12}(P(OPh)_3)_4]$ has been established [5,6]. PPh_3 has a larger cone angle than $P(OPh)_3$ [7] and it has been suggested [5] that a maximum of three PPh_3 ligands can be introduced by displacement of CO ligands from $[Rh_6(CO)_{16}]$.

Introduction of halide and pseudohalide ligands is limited to mono- and di-substituted species $[Rh_6(CO)_{15}X]^-$ (X = Cl, Br, I, CN, SCN, COOMe, COOEt, $CONH^iPr$) and $[Rh_6(CO)_{14}(CN)_2]^{2-}$ as a consequence of the strong donor ability of anionic ligands, which affects the electron density on the metal core [8]. Multidentate phosphorus ligands [9,10], dienes [11], arsines and bipyridine [12] have also been introduced by reaction with $[Rh_6(CO)_{16}]$. Hexanuclear Rh-clusters have also been obtained from $[Rh_4(CO)_{12}]$ in the case of dienes and anionic ligands, and from $[Rh_2(CO)_4Cl_2]$ in the case of PH_3-ligand [13]. When tertiary phosphines and phosphites are introduced into $[Rh_4(CO)_{12}]$ the substitution products $[Rh_4(CO)_{11}L]$, $[Rh_4(CO)_{10}L_2]$, $[Rh_4(CO)_9L_3]$ and $[Rh_4(CO)_8L_4]$ are obtained [14].

We have previously observed that SMe_2 is a versatile ligand in tetranuclear metal cluster compounds [15,16], as well as giving rise to an extensive chemistry in the case of mononuclear compounds [17]. In some of the cluster compounds SMe_2 is coordinated as a terminal ligand, which is unusual for sulphur ligands in cluster compounds. We describe below the results of a study of SMe_2 derivatives of a larger cluster $[Rh_6(CO)_{16}]$. The formation and crystal structures of SMe_2-substituted compounds of $[Rh_6(CO)_{16}]$, as well as their reactions with CO and H_2 are discussed.

Results and discussion

Synthesis and characterization of $[Rh_6(CO)_{16-x}(SMe_2)_x]$

$[Rh_6(CO)_{16}]$ reacts with dimethyl sulfide in refluxing THF to products up to the tetrasubstituted stage. With 1 : 1 – 1 : 1.4 cluster : ligand ratios and a 30 min reaction time $[Rh_6(CO)_{15}(SMe_2)]$ (**1**) and $[Rh_6(CO)_{14}(SMe_2)_2]$ (**2**) were obtained as the main products. With an excess of ligand and longer reactions, $[Rh_6(CO)_{13}(SMe_2)_3]$ (**3**) and $[Rh_6(CO)_{12}(SMe_2)_4]$ (**4**) were exclusively formed. The sulfide derivatives are significantly more soluble than the parent cluster.

The X-ray crystal structures of **1** and **4** have been determined. In these structures the sulfur ligands have replaced terminal carbonyls, leaving the parent cluster structure otherwise unchanged (see Figs. 1 and 2). In **4** the four sulfide ligands are bound to four rhodium atoms in the same plane, and lie alternately above and below the Rh_4 plane.

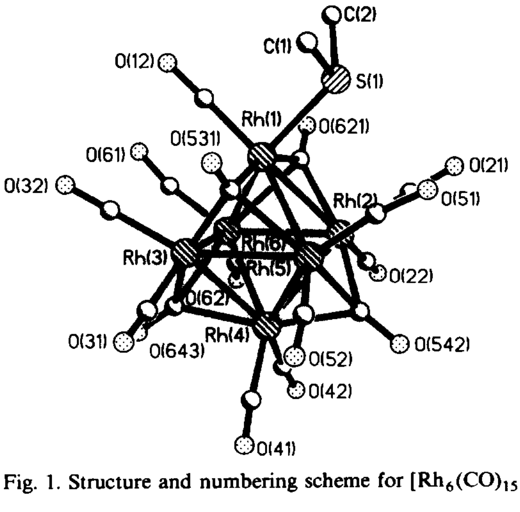

Fig. 1. Structure and numbering scheme for $[Rh_6(CO)_{15}(SMe_2)]$ (**1**).

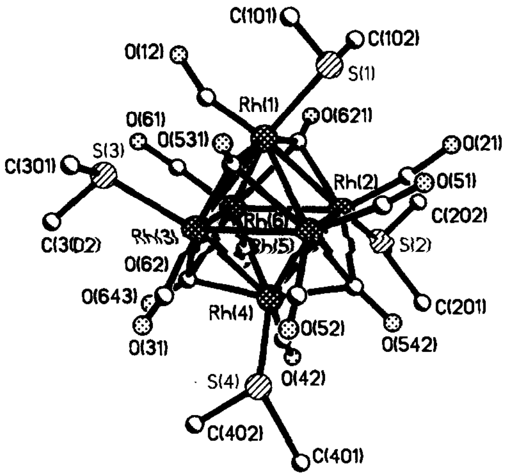

Fig. 2. Structure and numbering scheme for $[Rh_6(CO)_{12}(SMe_2)_4]$ (4).

Atomic coordinates are given in Tables 1 and 2, and selected bond lengths and selected bond angles in Tables 3 and 4. The average rhodium–rhodium bond lengths in **1** (271.2 pm) and **4** (276.2 pm) are close to those in $[Rh_6(CO)_{16}]$ [18] (278 pm) and $[PPN][RuRh_5(CO)_{16}]$ [19] (average M–M distance 276.9 pm).

In **4** the Rh–Rh distances depend slightly on the SMe_2 positions. The average (S–)Rh–Rh(–S) distance, 275.3 pm, is shorter than the average (S–)Rh–Rh (*cis* to the sulfide) distance, 281.6 pm, but it is longer than the average (S–)Rh–Rh (*trans* to the sulfide) distance, 271.8 pm. In **1** there is a corresponding difference between the *cis* (S–)Rh–Rh distances (274.0 pm) and *trans* (S–)Rh–Rh distances (271.8 pm). The Rh–Rh bonds with no SMe_2 ligands are slightly shorter (270.4 pm).

In $[Rh_6(CO)_{12}(P(OPh)_3)_4]$, in which the phosphite groups have similar arrangement as the sulfides in **4**, there is a similar difference between the Rh–Rh bonds *cis* (average 280.8 pm) and *trans* (average 275.4 pm) to the phosphite groups. However, the (P–)Rh–Rh(–P) bonds (average 281.3 pm) are longer than the others [6]. The Rh–C bond distances show no observable differences in compounds **1** and **4**.

In $[Rh_6(CO)_{12}(P(OPh)_3)_4]$ the bulky phosphite ligands cause crowding that apparently hinder the coordination of additional phosphites. With the much less bulky SMe_2 we obtained no evidence for derivatives containing five or six SMe_2 ligands, and so it is possible that electronic factors also limit the number of the substituents. Likewise with $[HRuCo_3(CO)_{12}]$ we obtained no evidence for trisubstituted SMe_2 derivatives, and even the disubstituted derivative decomposes readily, although the more crowded phosphine derivative $[HRuCo_3(CO)_9(PMe_2Ph)_3]$ is formed readily and is stable [20].

The C–Rh–C angles in $[Rh_6(CO)_{12}(P(OPh)_3)_4]$ are low (mean 88°) due to the crowding caused by the phosphite groups [6]. The average C–Rh–C and S–Rh–C angles of terminal carbonyls in **1** (92.6 and 90.7°) and **4** (92.8 and 93.7°) are similar to the corresponding C–Rh–C angles in $[PPN][RuRh_5(CO)_{16}]$ (average 93.2°), showing that the SMe_2 ligands cause no significant distortions in the structures of **1** and **4**. The similarity in coordination geometries of SMe_2 and CO ligands is also shown by the Rh–Rh–S and Rh–Rh–C angles (*cis*), which are very

Table 1

Atomic coordinates ($\times 10^3$) for [$Rh_6(CO)_{15}(SMe_2)$] (**1**)

Atom	*x*	*y*	*z*
Rh(1)	368.6(1)	186.6(4)	906.8(2)
Rh(5)	410.2(2)	388.6(4)	870.6(3)
Rh(4)	378.3(2)	285.5(5)	717.0(3)
Rh(3)	421.9(2)	117.9(5)	847.1(3)
Rh(2)	324.8(2)	358.2(5)	774.2(3)
Rh(6)	335.5(2)	90.0(4)	749.8(3)
S(1)	357.5(5)	314(1)	1005.5(9)
O(531)	467(1)	211(4)	1032(2)
O(542)	364(1)	588(4)	727(2)
O(621)	270(1)	159(4)	815(2)
O(643)	394(1)	−7(4)	680(2)
O(12)	372(1)	−78(4)	989(2)
O(21)	299(1)	56(3)	860(2)
O(22)	244(1)	391(4)	611(2)
O(31)	508(2)	141(4)	867(3)
O(32)	438(2)	−172(6)	907(3)
O(41)	453(1)	375(4)	694(2)
O(42)	319(1)	315(4)	542(3)
O(51)	406(1)	607(4)	981(2)
O(52)	492(1)	493(4)	890(2)
O(61)	324(1)	−191(5)	797(2)
O(62)	267(2)	48(5)	576(3)
C(531)	439(1)	219(5)	964(3)
C(542)	364(1)	482(4)	752(2)
C(621)	301(2)	193(5)	816(3)
C(643)	388(2)	62(6)	720(4)
C(12)	370(2)	230(6)	959(3)
C(21)	310(2)	485(5)	829(3)
C(22)	276(1)	383(4)	673(2)
C(31)	476(2)	131(6)	852(3)
C(32)	432(2)	−63(6)	883(3)
C(41)	426(2)	342(5)	703(3)
C(42)	341(2)	301(6)	606(4)
C(51)	407(2)	518(5)	938(3)
C(52)	461(2)	455(6)	886(4)
C(61)	330(1)	−85(5)	775(3)
C(62)	294(2)	66(6)	643(4)
C(1)	408(2)	298(6)	1105(3)
C(2)	319(2)	229(5)	1025(3)

similar in both **1** (97.8 and 97.5°, respectively) and **4** (97.0 and 97.8°, respectively). The Rh–Rh–P angles in [$Rh_6(CO)_{12}(P(OPh)_3)_4$] are slightly larger (average 102.3°).

During X-ray structural determination the Fourier map for the asymmetric unit of **4** showed additional electron density peaks that were interpreted as disordered solvent atoms. The solvent is possibly hexane, which was used in the crystallization, but there are some peculiarities in the C–C distances. The peaks are assigned as carbons C1–C6. Attempted refinement of these peaks was not successful. (As a consequence of the presence of a solvent in the crystals of **4** the observed carbon and hydrogen contents were high.)

Table 2

Atomic coordinates ($\times 10^3$) for $[Rh_6(CO)_{12}(SMe_2)_4]$ (4) [a]

Atom	x	y	z
Rh(1)	5122	305.8(4)	100
Rh(2)	636.7(3)	292.6(4)	81.2(3)
Rh(3)	451.1(3)	291.7(4)	−31.4(3)
Rh(4)	575.3(1)	306.8(4)	−61.5(1)
Rh(5)	544.5(4)	97.8(1)	24.9(4)
Rh(6)	544.2(4)	501.0(1)	24.5(4)
S(1)	537.0(8)	174(2)	216.6(7)
S(2)	736.1(7)	412(2)	77.6(9)
S(3)	347.7(9)	416(2)	−24(1)
S(4)	552.9(8)	169(2)	−166.4(8)
O(542)	686(2)	92(4)	−18(2)
O(531)	406(2)	71(4)	65(2)
O(621)	623(2)	522(3)	184(2)
O(643)	469(2)	511(5)	−139(2)
O(12)	414(2)	477(4)	157(2)
O(21)	702(3)	118(6)	215(2)
O(31)	377(2)	137(4)	−162(2)
O(42)	677(2)	486(5)	−113(3)
O(51)	604(2)	−122(2)	128(1)
O(52)	488(3)	−119(5)	−91(2)
O(61)	446(2)	720(4)	50(2)
O(62)	633(2)	718(4)	−22(2)
C(542)	636(2)	143(4)	−2(2)
C(531)	443(2)	154(5)	518(3)
C(621)	601(3)	469(5)	140(3)
C(643)	494(2)	437(4)	−89(2)
C(12)	451(3)	408(5)	125(2)
C(21)	684(2)	196(4)	154(2)
C(31)	407(3)	184(8)	−124(5)
C(42)	639(2)	417(3)	−98(1)
C(51)	586(2)	−40(5)	86(2)
C(52)	511(3)	−36(6)	−52(2)
C(61)	486(2)	634(3)	42(2)
C(62)	606(3)	644(7)	−12(3)
C(101)	459(2)	138(3)	235(1)
C(102)	590(4)	262(7)	272(2)
C(201)	795(2)	311(6)	30(3)
C(202)	782(5)	440(12)	158(6)
C(301)	286(2)	304(5)	−36(2)
C(302)	317(2)	498(6)	−103(2)
C(401)	626(3)	155(9)	−243(7)
C(402)	510(1)	273(3)	−244(1)
C(1)	2709	3549	155
C(2)	3004	3416	2433
C(3)	2992	3374	2884
C(4)	2962	2030	2923
C(5)	3363	2270	3328
C(6)	3129	2226	4084

---

[a] C(1)–C(6) denote peaks thought to arise from a molecule of hexane (see text).

Table 3

Bond lengths (pm) for $[Rh_6(CO)_{15}(SMe_2)]$ (**1**) and $[Rh_6(CO)_{12}(SMe_2)_4]$ (**4**)

	1	**4**
Rh(1)–Rh(5)	273.5(7)	280.8(6)
Rh(1)–Rh(3)	271.3(9)	274.6(6)
Rh(1)–Rh(2)	274.4(6)	274.4(7)
Rh(1)–Rh(6)	272.3(6)	272.2(7)
Rh(5)–Rh(4)	269.6(7)	282.1(6)
Rh(5)–Rh(3)	273.0(7)	272.2(7)
Rh(5)–Rh(2)	269.9(7)	271.4(7)
Rh(4)–Rh(3)	269.1(6)	274.9(7)
Rh(4)–Rh(2)	270(1)	277.1(6)
Rh(4)–Rh(6)	268.8(8)	271.4(7)
Rh(3)–Rh(6)	272.6(7)	282.3(7)
Rh(2)–Rh(6)	270.3(7)	281.3(7)
Rh(1)–S(1)	240(2)	240(1)
Rh(2)–S(2)		236(2)
Rh(3)–S(3)		248(2)
Rh(4)–S(4)		240(2)
Rh(1)–C(531)	222(5)	217(5)
Rh(1)–C(621)	219(4)	237(5)
Rh(2)–C(542)	204(5)	219(4)
Rh(2)–C(621)	214(6)	229(6)
Rh(3)–C(531)	219(5)	215(5)
Rh(3)–C(643)	214(6)	213(4)
Rh(4)–C(542)	215(5)	218(4)
Rh(4)–C(643)	220(6)	205(4)
Rh(5)–C(531)	224(4)	234(5)
Rh(5)–C(542)	220(4)	212(5)
Rh(6)–C(621)	236(6)	230(6)
Rh(6)–C(643)	223(8)	229(4)
Rh(1)–C(12)	185(6)	169(5)
Rh(2)–C(21)	184(6)	178(4)
Rh(2)–C(22)	185(3)	
Rh(3)–C(31)	189(8)	211(8)
Rh(3)–C(32)	184(6)	
Rh(4)–C(41)	193(7)	
Rh(4)–C(42)	184(5)	195(3)
Rh(5)–C(51)	182(6)	186(4)
Rh(5)–C(52)	182(8)	199(5)
Rh(6)–C(61)	181(5)	185(3)
Rh(6)–C(62)	182(6)	212(7)
S(1)–C(101)	185(4)	175(3)
S(1)–C(102)	180(7)	159(6)
S(2)–C(201)		196(6)
S(2)–C(202)		165(10)
S(3)–C(301)		164(4)
S(3)–C(302)		173(5)
S(4)–C(401)		237
S(4)–C(402)		185(3)
O(531)–C(531)	117(5)	117(7)
O(542)–C(542)	114(6)	124(7)
O(621)–C(621)	115(7)	101(6)
O(643)–C(643)	108(8)	123(5)
O(12)–C(12)	111(7)	129(7)
O(21)–C(21)	113(7)	138(6)

Table 3 (continued)

	1	**4**
O(22)–C(22)	117(4)	
O(31)–C(31)	105(9)	95(8)
O(32)–C(32)	113(8)	
O(41)–C(41)	109(8)	
O(42)–C(42)	106(6)	112(6)
O(51)–C(51)	119(7)	114(5)
O(52)–C(52)	113(9)	112(7)
O(61)–C(61)	116(7)	121(5)
O(62)–C(62)	116(7)	96(8)

Compounds **2** and **3** were isolated by TLC, and characterised by IR spectroscopy and elemental analysis. When the IR spectra (Fig. 3) of the four compounds **1–4** were compared in the ν(CO) region they were seen all to show the same number of bands of differing intensities. The frequencies decrease with an increasing degree of substitution. The IR spectra previously reported for other mono-tetra substituted derivatives of [$Rh_6(CO)_{16}$] have also such a trend, but the dependence of the frequency on the degree of substitution is not as pronounced as in the SMe_2-substituted derivatives [1–4,8–10].

A mixture of compounds **1–4** were also formed when tetranuclear [$Rh_4(CO)_{12}$] was used as a starting material. The reaction occured in CH_2Cl_2 within a few hours even at room temperature.

Reactions of [$Rh_6(CO)_{12}(SMe_2)_4$] with CO and H_2

The reactivity towards carbon monoxide of some clusters obtained by substitution of CO ligands in [$Rh_6(CO)_{16}$] has been studied. Phosphine and phosphite compounds seem to break down to mono-, di- and tetra-nuclear species [21], unlike [$Rh_6(CO)_{14}$(bipy)] and [$Rh_6(CO)_{12}(bipy)_2$] for which the reversibility of the substitution has been demonstrated [12]. The reactivity of [$Rh_6(CO)_{12}(SMe_2)_4$] (**4**) towards CO and H_2 was studied in various solvents (CH_2Cl_2, hexane and THF) in a temperature range of 21–69 ° C (Table 5) and monitored by FT-IR spectroscopy.

Under a CO atmosphere **4** even at ambient temperature undergoes ligand substitution within a few hours to afford, via the trisubstituted species, the disubstituted Rh_6 cluster **2**. Cluster **2** was observed to be partly converted into the monosubstituted species at 40 ° C in CH_2Cl_2. When the mixture of **1** and **2** obtained in this way was heated at 69 ° C in hexane under CO [$Rh_6(CO)_{16}$] separated as a black precipitate. These results are in contrast to those obtained for [$Rh_6(CO)_{12}\{P(OPh)_3\}_4$], which breaks down in the reaction with CO to give tri- and di-substituted tetranuclear clusters [21].

When solutions of [$Rh_6(CO)_{12}(SMe_2)_4$] were stirred at room temperature under an H_2 atmosphere some conversion into the trisubstituted form was observed. At 40 ° C **4** was shown by IR monitoring to give **2** and **3**, which were separated by TLC along with some unchanged starting compound. A similar mixture of **4**, **3** and **2** was also obtained at 60 ° C in THF; in addition a small amount of an unidentified brownish violet material was obtained by TLC. Prolonged heating of solutions of **4** above 40 ° C always results in formation of a brownish black precipitate, which is

Table 4

Selected bond angles (°) for $[Rh_6(CO)_{15}(SMe_2)]$ (**1**) and $[Rh_6(CO)_{12}(SMe_2)_4]$ (**4**)

	1	**4**
Rh(5)–Rh(1)–S(1)	97.5(4)	95.6(4)
Rh(2)–Rh(1)–S(1)	98.0(4)	98.4(4)
S(1)–Rh(1)–C(531)	97(1)	94(2)
S(1)–Rh(1)–C(621)	92(2)	99(1)
Rh(3)–Rh(1)–C(12)	99(2)	92(1)
Rh(6)–Rh(1)–C(12)	99(2)	90(2)
S(1)–Rh(1)–C(12)	91(2)	100(1)
Rh(1)–Rh(5)–C(51)	96(2)	106(1)
Rh(2)–Rh(5)–C(51)	96(2)	95(1)
Rh(4)–Rh(5)–C(52)	100(2)	96(2)
Rh(3)–Rh(5)–C(52)	98(2)	94(2)
Rh(5)–Rh(4)–C(41)	95(1)	
Rh(5)–Rh(4)–S(4)		94.9(4)
Rh(3)–Rh(4)–C(41)	98(1)	
Rh(3)–Rh(4)–S(4)		99.4(4)
Rh(2)–Rh(4)–C(42)	99(2)	102.6(7)
Rh(6)–Rh(4)–C(42)	98(2)	97.0(8)
Rh(5)–Rh(3)–C(31)	99(2)	97(2)
Rh(4)–Rh(3)–C(31)	98(2)	94(2)
Rh(1)–Rh(3)–C(32)	98(2)	
Rh(1)–Rh(3)–S(3)		95.5(5)
Rh(6)–Rh(3)–C(32)	96(2)	
Rh(6)–Rh(3)–S(3)		97.2(4)
Rh(1)–Rh(2)–C(21)	96(2)	102(2)
Rh(5)–Rh(2)–C(21)	96(1)	98(1)
Rh(4)–Rh(2)–C(22)	97(2)	
Rh(4)–Rh(2)–S(2)		97.2(5)
Rh(6)–Rh(2)–C(22)	95(1)	
Rh(6)–Rh(2)–S(2)		97.7(4)
Rh(1)–Rh(6)–C(61)	95(1)	96(1)
Rh(3)–Rh(6)–C(61)	99(1)	100.1(9)
Rh(4)–Rh(6)–C(62)	96(2)	90(2)
Rh(2)–Rh(6)–C(62)	101(2)	102(2)
Rh(1)–S(1)–C(101)	106(2)	106(1)
Rh(1)–S(1)–C(102)	111(2)	106(2)
C(101)–S(1)–C(102)	103(3)	118(3)
Rh(2)–S(2)–C(201)		113(2)
Rh(2)–S(2)–C(202)		110(4)
C(201)–S(2)–C(202)		106(4)
Rh(3)–S(3)–C(301)		108(2)
Rh(3)–S(3)–C(302)		108(2)
C(301)–S(3)–C(302)		94(2)
Rh(4)–S(4)–C(402)		110(1)
Rh(1)–C(531)–O(531)	133(5)	136(4)
Rh(5)–C(531)–O(531)	135(4)	122(4)
Rh(3)–C(531)–O(531)	136(4)	141(4)
Rh(5)–C(542)–O(542)	129(3)	144(3)
Rh(4)–C(542)–O(542)	130(4)	124(3)
Rh(2)–C(542)–O(542)	140(4)	127(3)
Rh(1)–C(621)–O(621)	135(4)	136(5)
Rh(2)–C(621)–O(621)	140(4)	133(4)
Rh(6)–C(621)–O(621)	128(4)	141(2)
Rh(4)–C(643)–O(643)	132(6)	137(4)

Table 4 (continued)

	1	4
Rh(3)–C(643)–O(643)	136(4)	132(3)
Rh(6)–C(643)–O(643)	135(5)	128(3)
Rh(1)–C(12)–O(12)	176(5)	161(3)
Rh(2)–C(21)–O(21)	178(2)	162(4)
Rh(2)–C(22)–O(22)	175(4)	
Rh(3)–C(31)–O(31)	169(6)	165(8)
Rh(3)–C(32)–O(32)	177(6)	
Rh(4)–C(41)–O(41)	179(5)	
Rh(4)–C(42)–O(42)	177(6)	173(3)
Rh(5)–C(51)–O(51)	177(5)	170(4)
Rh(5)–C(52)–O(52)	176(4)	171(5)
Rh(6)–C(61)–O(61)	172(5)	176(3)
Rh(6)–C(62)–O(62)	179(7)	171(7)

insoluble in normal organic solvents and is probably formed by thermal fragmentation of the Rh_6 cluster framework.

Heating a solution of **4** under a N_2 atmosphere at ambient temperature and at 60 °C gave results similar to those for the reaction with H_2 (see Table 5) and it seems that **4** does not react with H_2 but is converted at higher temperature into a mixture of **2–4** and to an insoluble solid in a purely thermal reaction. There is an equilibrium between the tetra- and tri-substituted forms which is shifted towards the less-SMe_2-substituted clusters as the temperature is raised owing to the high volatility (b.p. 38 °C) of SMe_2. Coordination at the free ligand sites by CO from other molecules leads eventually to a fragmentation of the cluster molecules, which becomes apparent in the formation of a black precipitate. We previously observed similar behavior for a mixed metal tetranuclear $RuCo_3$ cluster that also contained SMe_2 as a monodentate ligand [22].

Hydrogenation of 1-hexene catalyzed by $[Rh_6(CO)_{12}(SMe_2)_4]$

Catalytic hydrogenation of 1-hexene with **4** as a catalyst precursor was studied in the temperature range 20–60 °C at a H_2 pressure of 1 atm. The catalytic activity was compared with that of $[Rh_6(CO)_{16}]$ and of $[H_4Ru_4(CO)_{12}]$. Under similar conditions $[H_4Ru_4(CO)_{12}]$ has been shown to catalyze the hydrogenation of ethylene, an observation which has implications for the mechanism of metal cluster catalysis [23]. The rates of hydrogenation of 1-hexene in the present catalysis studies are shown as a function of substrate-to-complex molar ratio in Table 6. Cluster **4** shows no catalytic activity below 40 °C, but at 60 °C actively catalyzes the hydrogenation, the highest turnover number being about 2200 mol hexane/(mol catalyst precursor × h). $[Rh_6(CO)_{16}]$ shows a somewhat lower activity at 60 °C. At that temperature $[H_4Ru_4(CO)_{12}]$ does not catalyze hydrogenation of 1-hexene at all, but is active at 72 °C.

It is difficult to judge the actual nature of the catalytic process catalyzed by **4**, since in the temperature range used for the catalysis **4** is known from the studies of its reactions described above to be converted into clusters bearing fewer SMe_2 ligands, along with an insoluble solid. In two experiments the black insoluble solid was recovered and its activity in catalytic hydrogenation of 1-hexene in heptane was

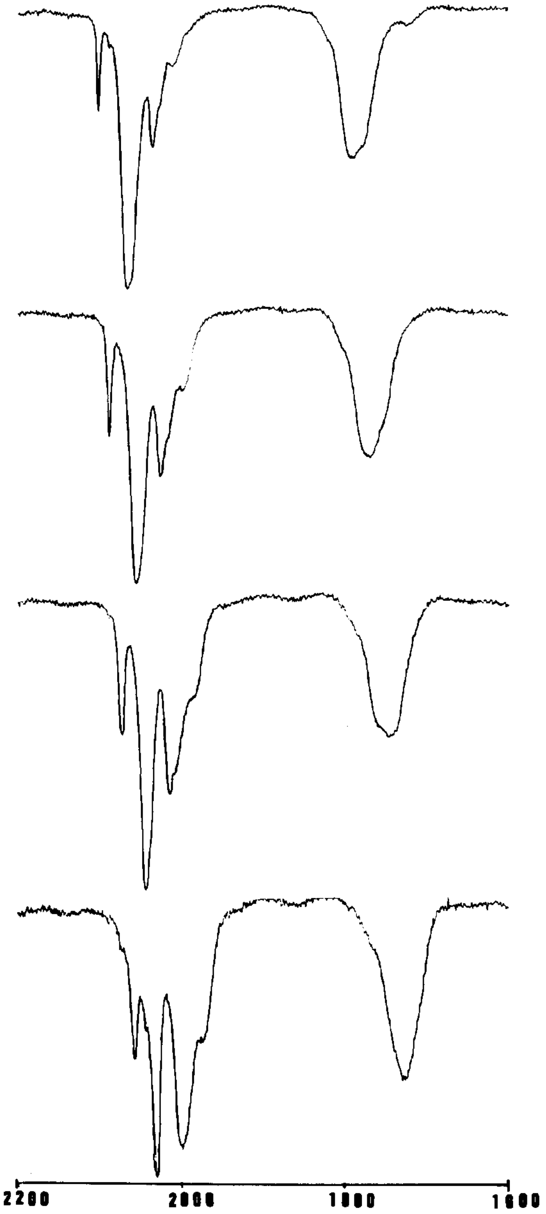

Fig. 3. Infrared spectra in the ν(CO) region for 1–4 in CH_2Cl_2.

examined. A hydrogenation rate of 29 mmol/h was observed, agreeing well with the rates of 30 and 29 mmol/h determined for 4 and $[Rh_6(CO)_{16}]$, respectively. This observation implies that the hydrogenation of 1-hexene by the present Rh_6 cluster precursors is heterogeneous in nature.

Experimental section

Except for chromatographic separations all manipulations were carried out under nitrogen. The SMe_2 was of commercial origin. $[Rh_6(CO)_{16}]$ was either of commercial

Table 5

Alteration of $[Rh_6(CO)_{12}(SMe_2)_4]$ to $[Rh_6(CO)_{12-n}(SMe_2)_n]$ (n = 1–4) in CO, H_2 and N_2 atmospheres as a function of temperature.

	21 °C/CH_2Cl_2	40 °C/CH_2Cl_2	60–69 °C/hexane or THF
CO	$n = 2$	$n = 2, 1$	$n = 1, 0$
H_2	$n = 4, 3$	n = 2, 3, 4 + i.s. [b]	n = 2, 3, 4 + i.s.
N_2	[a]	[c]	n = 3, 4 + i.s.

[a] no changes. [b] Insoluble solid. [c] Not studied.

origin or prepared as previously described [24]. THF was distilled from potassium-benzophenoneketyl. Chromatographic separations were carried out on silica plates with hexane–dichloromethane mixtures as eluents, since the separation on a silica column was incomplete.

The FT-IR spectra were recorded in an appropriate solvent on Nicolet 20SXC spectrometer.

For GLC analyses a Carlo Erba 4130 gas chromatograph, equipped with an FID detector and a CP-SIL 5CB capillary column, was used.

*Preparation of compounds **1–4***

$[Rh_6(CO)_{16}]$ (360 mg, 0.338 mmol) was dissolved in 50 ml of refluxing THF and dimethyl sulfide (150 μl, 2.116 mmol, cluster : ligand = 1 : 6) was added. The mixture was stirred for 30 min, the solvent then removed from the mixture under vacuum, and the residue chromatographed on silica plates with 1 : 1 hexane–dichloromethane as eluent to give: (i) $Rh_6(CO)_{15}(SMe_2)$ (**1**), yield 27 mg, 7%; (ii) $Rh_6(CO)_{14}(SMe_2)_2$ (**2**), yield 93 mg, 24%; (iii) $Rh_6(CO)_{13}(SMe_2)_3$ (**3**), yield 166 mg, 42%; and (iv) $Rh_6(CO)_{12}(SMe_2)_4$ (**4**), yield 30 mg, 7%.

Compounds **1** and **4** were recrystallized from 2:1 hexane dichloromethane mixture. IR (ν(CO) (cm^{-1}): **1**: 2102w, 2066vs, 2033w, 2008vw and 1792m; **2**: 2088w, 2055vs, 2027m, 2000w and 1772m; **3**: 2073m, 2044vs, 2016s, 1984m and 1749s; **4**: 2058w, 2032vs, 2002s, 1974m and 1729m (CH_2Cl_2). **1**: Found: C, 18.8; H: 0.6. $Rh_6C_{17}H_6O_{15}S$ calcd.: C, 18.6; H, 0.55%. **2**: Found: C, 19.2; H, 1.2. $Rh_6C_{18}H_{12}O_{14}S_2$ calcd.: C, 19.1; H, 1.1%. **3**: Found: C, 19.6; H, 1.6. $Rh_6C_{19}H_{18}O_{13}S_3$ calcd.: C, 19.5; H, 1.55%. **4**: Found: C, 26.7; H, 2.9. $Rh_6C_{20}H_{24}O_{12}S_4$ + C_6H_{14}(hexane) calcd.: C, 24.2; H, 3.0%.

Table 6

Rates of catalytic hydrogenation of 1-hexene [a]

Catalyst precursor	Substrate to complex mole ratio	T (°C)	Rate [b] (h^{-1})
$Rh_6(CO)_{12}(SMe_2)_4$	1800:1	20–40	0.0
	1800:1	60	2200
	460:1	60	1800
$Rh_6(CO)_{16}$	980:1	60	1200
$H_4Ru_4(CO)_{12}$	710:1	60	0.0
	710:1	72	74

[a] p_{H_2} = 1 atm., heptane solution = 20–30 ml. [b] Rate is reported as moles of substrate reduced per mol of complex per hour.

Preparation of $Rh_6(CO)_{15}(SMe_2)$ (1) and $Rh_6(CO)_{14}(SMe_2)_2$ (2)

$[Rh_6(CO)_{16}]$ (200 mg, 0.188 mmol) was refluxed in THF with SMe_2 (20 μl, cluster : ligand = 1 : 1.4) for 30 min. The yield of substituted species was 88%. The main component was **2** with **1** and only a small amount of **3** was present.

Preparation of $[Rh_6(CO)_{13}(SMe_2)_3]$ (3) and $[Rh_6(CO)_{12}(SMe_2)_4]$ (4)

Clusters **3** and **4** were prepared from 150 mg of $[Rh_6(CO)_{16}]$ and 1 ml of SMe_2 in refluxing THF during 3.5 h reaction. Chromatographic separation gave **3** (17 mg, 10%) and **4** (102 mg, 60%).

Preparation of 1–4 from $[Rh_4(CO)_{12}]$

Reaction between $[Rh_4(CO)_{12}]$ (80 mg, 0.107 mmol) and SMe_2 (785 μl, 10.7 mmol) in CH_2Cl_2 at room temperature for 2 h gave **1** in 9% yield, a mixture of **2** and **3** in 29% yield, and **4** in 18% yield.

Reactions of $[Rh_6(CO)_{12}(SMe_2)_4]$ (4) with H_2 or CO

The reactions of **4** with H_2 or CO or N_2 were carried out in a 100 ml flask. Typically a saturated solution of **4** was prepared in a degassed solvent (CH_2Cl_2, THF or hexane) and the flask charged with the gas to a slightly above one atmosphere pressure using a mercury bubbler. The reactions were first studied at ambient temperature for several hours and then at higher temperatures (normally at the reflux temperature of the solvent). The reactions were monitored by taking samples for IR-characterization. The products in the reaction mixtures were separated by thin layer chromatography and characterized by IR spectroscopy.

Catalytic hydrogenation of 1-hexene by $Rh_6(CO)_{12}(SMe_2)_4$

Compound **4** was weighed into a 100 ml reaction vessel and 20–30 ml of dried and deoxygenated heptane was added. The vessel, which was equipped with a reflux condenser, was evacuated and then charged with H_2 to 1 atm. The vessel was heated to the chosen reaction temperature in an oil-bath and the solution allowed to stand at that temperature for 15 min before 1 ml of 1-hexene was added from a syringe. The extent of hydrogenation of 1-hexene was monitored semiquantitatively by taking samples with a syringe from the reaction mixture for IR analysis; and observing the extent of disappearance of the C=C stretching frequency at 1642 cm^{-1}. That hydrogenation of 1-hexene had taken place was confirmed by GLC after the reaction had been stopped.

Crystallographic studies

Data were collected on a Nicolet R3m diffractometer using Mo-K_α radiation (λ = 0.71073 Å). Intensities were corrected for background, polarisation, and Lorenz effects. Empirical absorption correction was made from ψ-scan data for **4**. Table 7. gives further details.

The metal atom positions were determined by direct methods by use of the SHELXTL program package [25]. All remaining non-hydrogen atoms were located by the usual combination of full-matrix least-squares refinement and difference electron syntheses. Rhodium and sulfur atoms were anisotropically refined in the case of **1**; in the case of **4** anisotropic refinement was carried out for all non-hydrogen

Table 7

Crystallographic data for $[Rh_6(CO)_{15}(SMe_2)]$ (1) and $[Rh_6(CO)_{12}(SMe_2)_4]$ (4)

	1	**4**
M	1099.74	1202.09
Crystal system	Monoclinic	Monoclinic
Space group	$C2/c$	Cc
a, Å	35.73(1)	20.444(7)
b, Å	9.712(4)	9.764(4)
c, Å	18.559(9)	19.589(9)
β, deg	119.13(3)	104.27(3)
V, Å^3	5626(4)	2790(2)
Z	8	4
D_{calc}, g cm^{-3}	2.60	2.11
Centering 2θ, deg	13–21	15–24
Centering refl	25	23
2θ limits, deg	4–50	5–50
hkl range	43, 12, ±23	25, 12, ±24
$F(000)$	4112	1980
No. of unique reflections	4943	3422
No. of observed data,		
$I > 3\sigma(I)$	1130	2745
μ, mm^{-1}	3.52	2.61
No. of parameters	192	377
R [a]	0.0675	0.0361
R_w [b]	0.0618	0.0361

[a] $R = \Sigma||F_o| - |F_c||/\Sigma|F_o|$. [b] weight $= 1/(\sigma^2(F) + 0.0005F^2)$.

atoms. Methyl protons were placed in idealized positions (C–H = 0.96 Å, $U = 0.08$ Å^2) and not refined.

The structure of **4** was also refined in the centrosymmetric space group $C2/c$. This refinement led to a significantly higher R value (5.2%) and furthermore electron density peaks were generated near the metal atoms and two of the methyl carbons did not refine well ($U_{eq} = 0.32$ for C(201) and $U_{eq} = 0.62$ for C(202)).

Tables of anisotropic thermal parameters and bond lengths and angles for **1** and **4** and lists of for structure factors are available from the authors.

References

1 G. Wilkinson, F.G.A. Stone and E.W. Abel (Eds.), Comprehensive Organometallic Chemistry, Vol. 5, Pergamon, Oxford, 1982, p. 327.

2 K. Iwatate, S.R. Dasgupta, R.L. Schneider, G.S. Smith and K.L. Watters, Inorg. Chim. Acta, 15 (1975) 191.

3 B.L. Booth, M.J. Else, R. Fields and R.N. Haszeldine, J. Organomet. Chem., 27 (1971) 119.

4 B.F.G. Johnson, J. Lewis and P.W. Robinson, J. Chem. Soc. (A), (1970) 1100.

5 G. Ciani, L. Garlaschelli, M. Manassero, U. Sartorelli and V.G. Albano, J. Organomet. Chem., 129 (1977) C25.

6 G. Ciani, M. Manassero and V.G. Albano, J. Chem. Soc., Dalton Trans., (1981) 515.

7 C.A. Tolman, Chem. Rev., 77 (1977) 313.

8 P. Chini, S. Martinengo and G. Giordano, Gazz. Chim. Ital., 102 (1972) 330.

9 K. Nomiya and H. Suzuki, J. Organomet. Chem., 168 (1979) 115.

10 A. Ceriotti, G. Ciani, L. Garlaschelli, U. Sartorelli and A. Sironi, J. Organomet. Chem., 229 (1982) C9.

11 Z. Hou, Y. Wakatzuki and H. Yamazaki, J. Organomet. Chem., 399 (1990) 103.

12 K. Nomiya and H. Suzuki, Bull. Chem. Soc. Jpn., 52 (1979) 623.

13 F. Klanberg and E.L. Mutterties, J. Am. Chem. Soc., 90 (1968) 3296.

14 B.T. Heaton, L. Longhetti, D.M.P. Mingos, C.E. Briant, P.C. Minshall, B.R.C. Theobald, L. Garlaschelli and U. Sartorelli, J. Organomet. Chem., 213 (1981) 333.

15 S. Rossi, J. Pursiainen, M. Ahlgren and T.A. Pakkanen, Organometallics, 9 (1990) 475.

16 S. Rossi, J. Pursiainen and T.A. Pakkanen, Organometallics, 10 (1991) 1390.

17 M.A. Weiner and M. Lattman, Inorg. Chem., 17 (1978) 1084.

18 E.R. Corey, L.F. Dahl and W. Beck, J. Am. Chem. Soc., 85 (1963) 1202.

19 J. Pursiainen, T.A. Pakkanen and K. Smolander, J. Chem. Soc., Dalton Trans., (1987) 781.

20 J. Pursiainen, S. Rossi, T.A. Pakkanen, unpublished results.

21 A. Ceriotti, L. Garlaschell, G. Longoni, M.C. Malatesta, D. Strumilo, A. Fumagalli and S. Martinengo, J. Mol. Catal., 24 (1984) 309.

22 K. Kallinen, T.T. Pakkanen, J. Pursiainen and T.A. Pakkanen, VII International Symposium on Homogeneous Catalysis, Lyon, France, 1990.

23 Y. Doi, K. Koshizuka and T. Keii, Inorg. Chem., 21 (1982) 2732.

24 P. Chini and S. Martinengo, Inorg. Chim. Acta, 3 (1969) 315.

25 SHELXTL PLUS, Release 3.4, Nicolet Co., Madison, WI, 1988.